e-ISSN: 2349-9745
p-ISSN: 2393-8161

Scientific Journal Impact Factor (SJIF): 1.711

International Journal of Modern Trends in Engineering and Research

www.ijmter.com

IMPROVEMENT IN MORPHOLOGICAL AND ELECTRO-MAGNETIC BEHAVIOUR OF HARD FERRITE PERMANENT MAGNETS BASED ON Ni-Ir SUBSTITUTION

Ekta Chaturvedi[a], K. G. Rewatkar[b], V. M. Nanoti[c]

[a]*Department of Physics, Priyadarshini College of Engineering, Nagpur, India*
[b]*Department of Physics, Dr. Ambedkar College, Dikshabhoomi, Nagpur, India*
[c]*Department of Physics, Priyadarshini Institute of Engineering and Technology, Nagpur, India*

Abstract---The Ni-Ir substituted strontium ferrite of $Sr(Ni\text{-}Ir)_xFe_{12-2x}O_{19}$ (x = 0.02 & 0.08) were synthesized by sol-gel auto combustion technique and characterized using X-ray diffraction (XRD), Transmission Electron Microscopy (TEM) for morphological behaviour with electrical characteristics using Impedance Analyzer. XRD results confirmed the formation of a single phase M-type hexagonal unit cell of space group $P6_3/mmc$. The increase in Ni-Ir concentration increases the lattice parameter. TEM analysis of the sample demonstrates the formation of nano-size particles which decreases with substitution. In this paper we reported the variation of dielectric constant, dielectric loss, tangent loss, conductivity and magnetic behaviour with composition with temperature and frequency analysis of the sample. The migration of Fe^{3+} ion from octahedral to tetrahedral site decreases the dielectric constant with increase in Ni-Ir concentration. Activation energies were found similar with calculated at ferromagnetic and paramagnetic region. The material study we confined that the activation energy in the paramagnetic region is higher than that in the ferromagnetic region. The enhanced resistivity of Ni-Ir substituted strontium hexaferrites is a prospective application in high frequency and in microwave devices development.

Keywords: Electro-magnetic behaviour, Sol–gel auto-combustion technique, magnetoplumbite, Dielectric loss, Activation Energy etc.

I. INTRODUCTION

Ferrites-oxides have remarkable magnetic properties; have been investigated and applied during the last 50 years with a little improvement in their magnetic properties is of great importance [1]. The M-type ferrite crystallizes in a hexagonal structure with 64-ions per unit cell on 11 different symmetry sites. The 24 Fe^{3+} atoms are distributed over a distinct sites: three octahedral sites (12k, 2a, 4f2), one tetrahedral (4f1) site and one trigonal bi-pyramidal site (2b) [2].

The structural, morphological, electrical, dielectric and magnetic properties of hexaferrites depend upon the method of preparation, composition, concentration and distribution of the substituted cations at the five crystallographic sites. The preparation of hexaferrites is materialised by the sol–gel auto-combustion method is used to speed up the synthesis of complex materials. It is a simple process, a significant in time saving and energy consumption over the traditional methods. Small crystalline size of the resultants have an important influence on the particles of the prepared materials. This method is employed to obtain improved material powder characteristics, more homogeneity and have a minimum particle size, thereby influencing structural, electrical, and magnetic properties of hexagonal ferrites. Several cations combinations such as Ir^{4+}-Zn^{2+} [3], Ti^{4+}-M^{2+} (M= Mn, Ni, Zn, Co) [4], Ti^{4+}-Mg^{2+} [5] have been attempt by several researchers in order to improve the magnetic and electrical properties of strontium hexaferrites. In this reaserch paper we

report the effect of Ni-Ir substitution on structure, morphology and electro-magnetic behaviour of strontium nano-hexferrite prepared by sol-gel auto combustion method.

II. EXPERIMENTAL DETAILS:

2.1 Synthesis

$Sr(Ni\text{-}Ir)_xFe_{12-2x}O_{19}$ (x = 0.02 and 0.08) is prepared through sol-gel autocombustion technique which has emerged as a facile and economically viable technique in the preparation of nanomaterials. The sol-gel is produced by dissolving precursors as $Sr(NO_3)_2$, $Ni(NO_3)_2.6H_2O$, $IrBr_4$, $Fe(NO_3)_3.9H_2O$ and $CO(NO_3)_2.6H_2O$ in unionized water with the weight concentration. The fuel use in this combination is urea as reducing agent to supply requisite energy to initiate exothermic reaction amongst oxidants. The solution is then heated to transform precursor solution into gel formation of the solution. The complete process is carried out for about 20-30 minutes till complete homogenous thick gel is produced [6]. This homogenous gel is then allowed to fire in microwave oven of 2.45 GHz in presence of water molecule and excessive oxygen which is digitally programmed to produce 'as-burned sample'. The gel after firing converts in homogenous nano-crystalline powder. The sample is then grinded in three cycles using pestle and mortar to make it more fine and ultrafine tend to produce nano-hexaferrite. The polyvinyl alcohol solution (2-3 drops) has been mixed before they palletized by hydraulic press using stainless steel die set under uni-axial appropriate pressure for 15 min. The Polyvinyl Acetate has been used as a binder. The pellets of the sample have been calcined at 800^oC for about 4 hrs in the electric furnace to obtained M-type strontium hexaferrites. The prepared samples are then stored in air tight containers by sealing them [7].

2.2 Characterization

The structure and phase purity of these samples is investigate with XRD at room temperature using (Bruker Kappa Apex II D8 advance, Cu Kα radiation λ = 0.1540 nm) in continuous scanning mode and the structural parameters like lattice constants (a and c), interplanar spacing (d), crystallite size (D), miller indices (h k l), X-ray density (ρ_x), bulk density (ρ_{bulk}), porosity (P), were calculated. The detailed information on the morphology and verify the particle size of Ni-Ir substituted hexaferrites, a set of micrographs were taken by TEM-CM200 at the operating voltage of 20-200 KV with the resolution of 2.4 Å. The magnetization (M) versus magnetic field (H) measurement of studied powder material was carried out by Vibrating sample Magnetometer (VSM) (Lakeshore 665). The idea of VSM is based on the Faraday induction law. Their magnetic moment, saturation magnetization (M_s), remnant magnetization(M_r), coercivity(H_c), SQR etc have been measured and studied. The electrical and dielectric studies for the pelletized sample were carried out between temperatures 30^oC to 350^oC in the frequency range 100 Hz to 10 MHz using precision Impedance Analyzer (6500B, Waynekar electronics). The pellets were coated with air-drying silver paint for proper electrical contact. It uses four-lead measurement technique for the best possible accuracy in the measurement.

III. RESULTS AND DISCUSSION

3.1 X-Ray diffraction studies

The X-ray diffraction patterns of samples are taken with X-ray diffraction-meter and Cu-Kα radiation with wavelength λ = 0.1540 nm shown in figure (1). Using 2θ, observed d-values and intensity calculations, d-value is calculated and (h k l) planes are confirmed. The values shown in table 1(a) and (b) confirm the formation of single phase hexagonal ferrite with space group $P6_3/mmc$. The lattice parameter 'a', 'c' and volume 'V' for each sample has been calculated using the relation.

$$\frac{1}{d_{hkl}^2} = \frac{4}{3}\left(\frac{h^2+hk+k^2}{a^2}\right) + \frac{l^2}{c^2} \qquad (1)$$

$$V = 0.866a^2 c \quad (2)$$

Where (h k l) are Miller (reflection) indices of the plane whose interplanar spacing is d_{hkl}. On substituting Ni^{2+} and Ir^{4+} ions in $SrFe_{12}O_{19}$, the effect of the variation of Ni-Ir substitution on the lattice parameters a, c as well as on D, V, ρ_x, ρ_{bulk} and P are summarized in Table 2. It is found that the lattice constant of the ferrite phase (hexagonal) increases with increasing Ni-Ir contents, in strontium ferrite substitution. This is attributed to larger ionic radii of Ni^{2+} (0.72 A°) and Ir^{4+} (0.68 Å) than Fe^{3+} ion (0.64 Å) [8]. The X-ray densities (ρ_{xray}) for the samples are tabulated in Table 2 which is calculated using the equation

$$\rho_{xray} = ZM/NV \quad (3)$$

Where 'M' is the molar mass of the sample, 'N' is Avogadro's number, 'Z' is a number of molecules (Z = 2 for M-type hexaferrite) and 'V' is the volume of the cell, calculated from equation (2). The bulk density ρ_{bulk} values were observed to be lesser than the corresponding X-ray density values which is attributed to the generation of unavoidable pores due to composite combination during sintering process. Similar observation has been reported by Vaishali V. Soman et.al. [5]. It is further observed that with the increase in x, ρ_{xray} and P decreases. The crystalline size for each composition is calculated from XRD line width using Scherer formula shown in table (2)

$$D = k\lambda/h\cos\theta \quad (4)$$

Where D is average size of the crystallites, k is Scherer constant (0.9), λ is wavelength of radiation (1.54056Å) and h is peak width of half height (FWHM). It is observed that the value of particle size decreases with the substitution of Ni-Ir in $SrFe_{12}O_{19}$ matrix. This observation can be correlated to the XRD micrographs given in Figs. 1 (a)–(b).

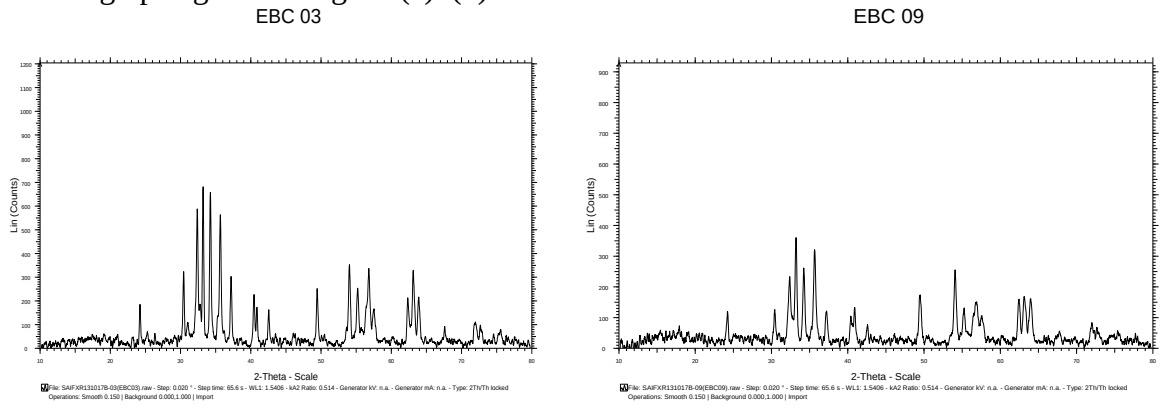

Fig.1: XRD spectrum of (a) $Sr(Ni\text{-}Ir)_{0.02}Fe_{11.96}O_{19}$ and (b) $Sr(Ni\text{-}Ir)_{0.08}Fe_{11.84}O_{19}$

Table 1: X-ray diffraction data (A) Sr $(Ni\text{-}Ir)_{0.02}Fe_{11.96}O_{19}$ and (B) Sr$(Ni\text{-}Ir)_{0.08}Fe_{11.84}O_{19}$

S.no.	2θ	d_{obs}	d_{cal}	I/I_o(%)	h, k, l
1	24.16	3.679	3.679	26.9	0 0 6
2	30.40	2.937	2.906	47.2	1 1 0
3	32.03	2.766	2.759	86.3	0 0 8
4	33.17	2.698	2.672	100	1 0 7
5	34.57	2.591	2.571	96.5	1 1 4
6	35.63	2.517	2.517	82.6	2 0 0
7	37.16	2.416	2.419	44.2	1 0 8
8	40.85	2.207	2.207	33	0 0 10
9	42.55	2.123	2.137	23.5	1 1 7
10	49.46	1.841	1.842	36.7	2 1 3
11	54.07	1.694	1.690	51.6	2 1 6
12	55.38	1.657	1.659	36.9	3 0 2
13	56.48	1.627	1.629	28.4	2 1 7
14	57.54	1.600	1.605	49.2	3 0 4
15	62.40	1.486	1.485	30.9	2 0 12
16	63.20	1.470	1.471	48.1	0 0 15
17	63.98	1.454	1.453	31.4	2 2 0
18	67.69	1.383	1.384	13.1	3 0 9
19	72.06	1.311	1.312	15.9	1 1 15
20	72.76	1.298	1.298	13.9	0 0 17

S.no.	2θ	d_{obs}	d_{cal}	I/I_o(%)	h, k, l
1	23.88	3.722	3.728	32.9	0 0 6
2	30.36	2.941	2.910	34.5	1 1 0
3	32.14	2.782	2.796	41.1	0 0 8
4	33.16	2.698	2.698	100	1 0 7
5	34.65	2.586	2.581	72.3	1 1 4
6	35.59	2.520	2.520	89	2 0 0
7	37.11	2.420	2.431	33.2	1 1 5
8	40.54	2.223	2.229	21.8	1 0 9
9	42.55	2.122	2.151	20.9	1 1 7
10	49.38	1.843	1.845	47.2	2 1 3
11	54.05	1.695	1.696	70.6	2 1 6
12	55.24	1.661	1.661	36.1	3 0 2
13	57.30	1.606	1.609	21.5	3 0 4
14	62.44	1.486	1.487	44	3 0 7
15	63.13	1.471	1.481	46.4	1 1 13
16	63.96	1.454	1.452	44.2	2 2 1
17	72.02	1.310	1.315	22.7	0 0 17

Table 2: Structural parameters of $Sr(Ni\text{-}Ir)_xFe_{12-2x}O_{19}$

S. no.	Composition X	Particle Size (nm)	Lattice Constant (Å)		Volume $(Å)^3$	ρ_{xray} (gm/cm^3)	ρ_{bulk} (gm/cm^3)	Porosity (%)
1	0.02	39.18	5.8133	22.074	646.01	5.47	2.92	46.48
2	0.08	25.22	5.8203	22.369	656.25	5.42	3.13	42.17

3.2 Transmission Electron Microscopy (TEM) studies

The particle size is determined with the TEM studies [9]. TEM photograph of the sample are shown in Figure 2(a)-(b). The size is found to be 32 nm confirming the nano size particle formation of the hexaferrites. The grains are found to be hexagonal platelets. The average grain size is further found to be reduced as the value of x increases from 0.02 to 0.08. It is reasonable to confirm that the doping of divalent and tetravalent ions does remain responsive to the particle size of the substituted hexaferrite [10].

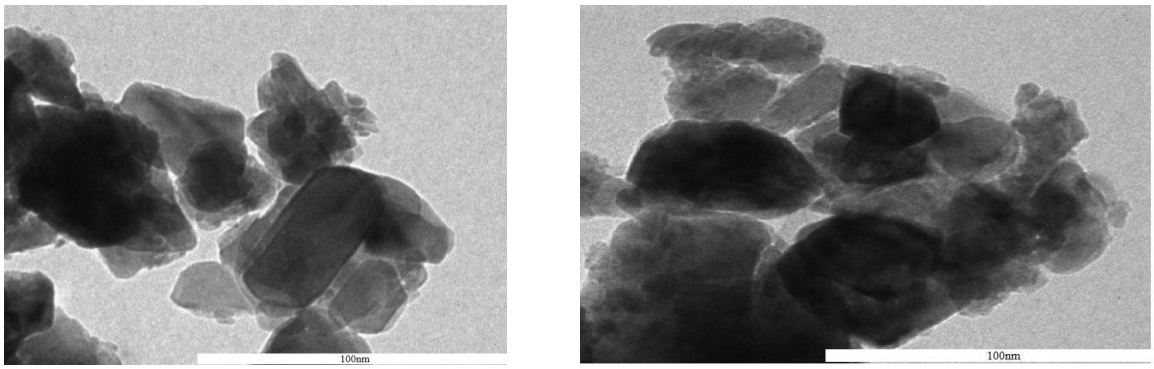

Fig 2: TEM pictures of (a) $Sr(Ni\text{-}Ir)_{.02}Fe_{11.96}O_{19}$ and (b) $Sr(Ni\text{-}Ir)_{.08}Fe_{11.84}O_{19}$

3.3 Electrical Properties

3.3.1 Variation of tangent loss (tanδ) with frequency and temperature

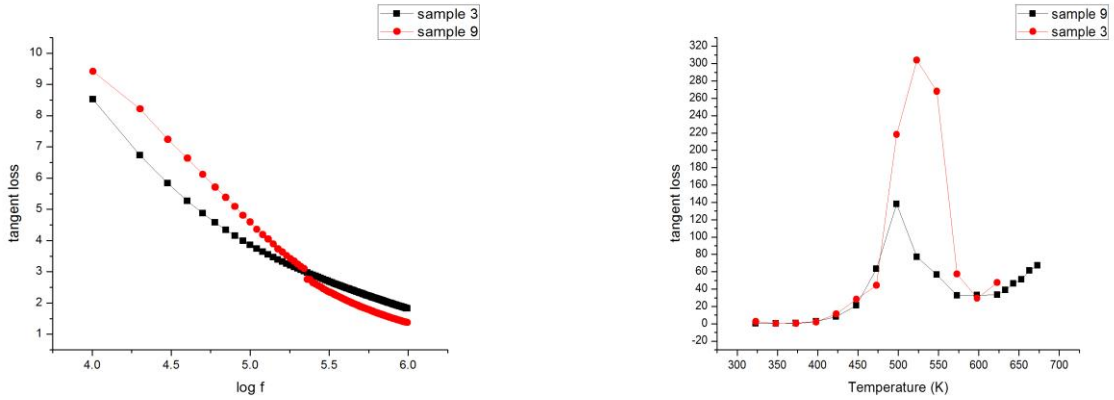

Fig. 3: Variation of tangent loss (tanδ) with frequency and temperature

3.2 Variation of conductivity (σ) with frequency and temperature:

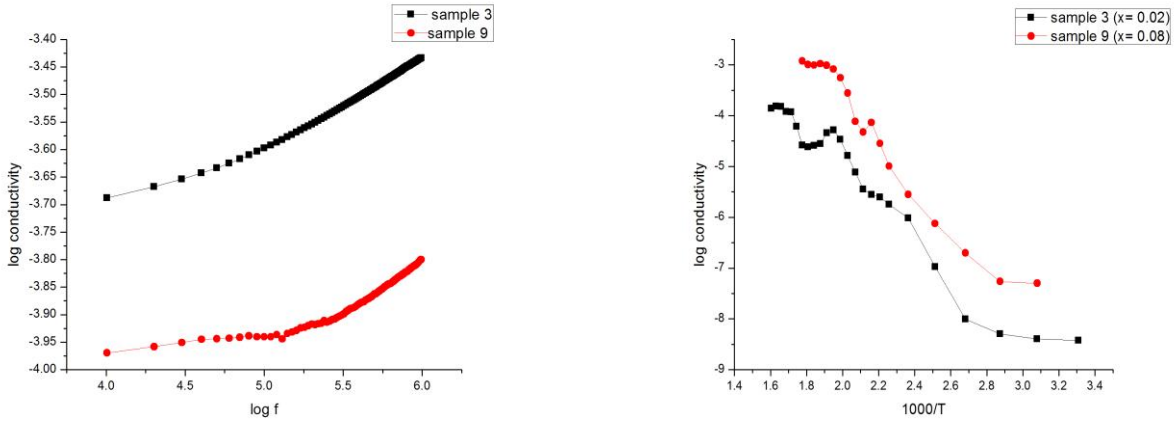

Fig. 4: Variation of conductivity (σ) with frequency and temperature

3.3.3 Variation of dielectric constant (ε') with frequency and temperature:

The dielectric properties of ferrite nanoparticles are influenced mainly by the synthesis technique, grain size, cation distribution etc. The dielectric constant (ε') is calculated by using the formula

$\varepsilon' = cd/\varepsilon_o A$ (5)

where 'c' is the capacitance, 'd' is the thickness of the sample, 'A' is the area of cross-section and 'ε_o' is the permittivity of free space. Figure 5 (a) displays the variation of dielectric constant ε', as a function of frequency at room temperature from 100 Hz–10MHz It is observed that at low frequencies, ε' has high values and in general ε' decreases with increase in frequency, showing dispersion in low frequency range. All the sample show dispersion which can be explained by Koops (1951) [11] on the basis of Maxwell-Wagner (1913) two layer model [12]. The decrease in dielectric constant with increasing frequency is attributed to the electron exchange between Fe^{2+} and Fe^{3+} ions cannot follow the change of the external applied field beyond certain frequency. This decreases the probability of electrons reaching the grain boundaries and as a result polarization decreases [13]. The decrease of the dielectric constant, ε′, with Ni-Ir ions substitution can be explained on the basis of migration of Fe^{3+} ions from octahedral site to tetrahedral site. This decreases the hopping and hence decreases the polarization for x = 0.08.

The variation of ε′ with temperature is shown in Figure 5 (c)-(d) where the dielectric constant increases gradually with increase in temperature up to a certain temperature designated as dielectric transition temperature (T_d). However beyond this temperature, the values of the dielectric constant were found to decrease gradually. It has been found that T_d for $Sr(Ni\text{-}Ir)_{.02}Fe_{11.96}O_{19}$ is 603K and for $Sr(Ni\text{-}Ir)_{.08}Fe_{11.84}O_{19}$ it is 623K. A similar temperature variation of dielectric constant has been reported by Vaishali V. Soman et.al. [14]. This change in ε' beyond T_d is attributed to the magnetic transition from ordered (ferromagnetic) to disordered (paramagnetic) state. The increase in ε' with temperature can be explained on the basis that as the temperature increases the hopping between Fe^{2+} and Fe^{3+} ions on the octahedral sites is thermally activated. This hopping causes local displacement in the direction of external electric field which increases the space charge polarization and hence ε' also increases. However beyond the transition temperature, the ions and electron are less oriented towards the field direction and hence the dielectric constant decreases.

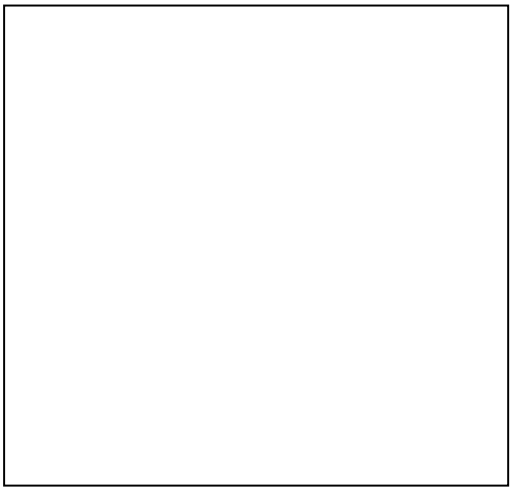

(a)

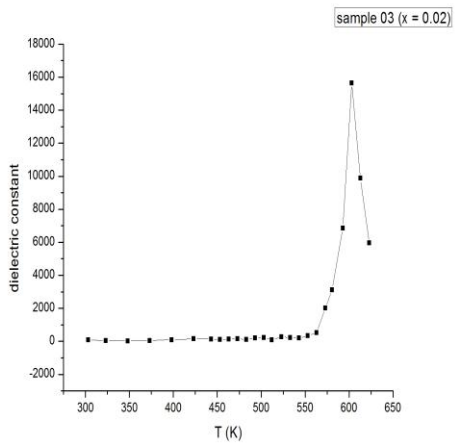

(b)

Fig. 5: (a) variation of dielectric constant with frequency at room temperature for $Sr(Ni\text{-}Ir)_xFe_{12-2x}O_{19}$ (x = 0.02 and 0.08) (b) variation of dielectric constant with temperature at constant frequency for $Sr(Ni\text{-}Ir)_{.02}Fe_{11.96}O_{19}$ (c) for $Sr(Ni\text{-}Ir)_{.08}Fe_{11.84}O_{19}$

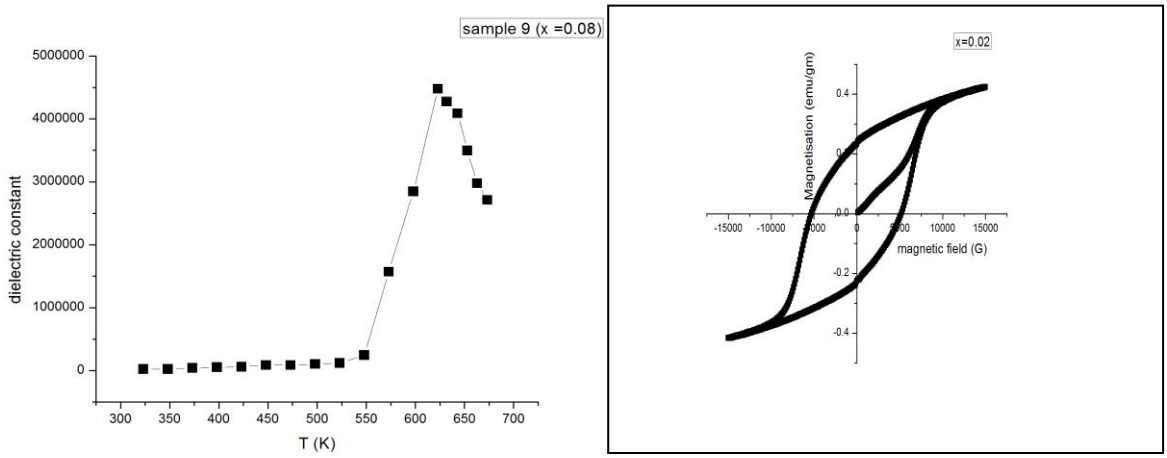

DISCUSSION

The bulk density ρ_{bulk} values were observed to be lesser than the corresponding X-ray density values which is attributed to the generation of unavoidable pores due to composite combination during sintering process. With the material study we confined that the activation energy in the paramagnetic region is higher than that in the ferromagnetic region. The enhanced resistivity of Ni-Ir substituted strontium hexaferrites is a prospective application in high frequency and in microwave devices development.

ACKNOWLEDGMENT

The author would express their thanks towards the nano material development group and research member of Nagpur. Also toward the Dr. Ambedkar College, Nano-Technology Department for providing necessary characterisation instrumentation and Mr. Anup Bhat for encouragement and supporting and directing towards completion of this paper.

REFERENCES

[1] Lechevallier, L., J. M. Le Breton, J.F. Wang and I.R. Harris, Journal of Magnetism and Magnetic Materials **269** (2004).
[2] Naeem Ashiq, M., M. Javed Iqbal and I. Hussain Gul, Journal of Alloys and Compounds 487 (2009).
[3] M.J. Iqbal, M.N. Ashiq, P.H. Gomez, Journal of Alloys Compound 478 (2009) 736.
[4] Q.Q. Fang, Y.M. Liu, P. Yin, X.G. Li, Journal of Magnetism and Magnetic Materials 234 (2001) 366.
[5] Vaishali V. Somana, V. M. Nanoti, D.K. Kulkarni, Ceramics International 39 (2013) 5713–5723.
[6] David W. Oxtoby, Alan Campion, H. P. Gillis, Principles of Modern Chemistry (6th Edition), April 2007.
[7] Kristi Lew, Chemical Reaction (1st Edition), March 2008.
[8] S. Kanagesan, M. Hashim, T. Kalaivani, I. Ismail and N. Rodziah, World Applied Sciences (5) (2014).
[8] K. G. Rewatkar, N. M. Patil, S. R. Gawali, Bulletin of materilas Science 28 (6) (2005) 585-587.
[9] S. N. Sable, K. G. Rewatkar, V. M. Nanoti, Journal of Material Science and Engineering B 168 (2010).
[10] C. G. Koops, Physical review 83 (1951).
[11] K. W. Wagner, Annals of Physics (Leipzig) 40 (1913) 817.
[12] G. Sathishkumar, C. Vankataraju, K. Sivakumar, Materials Sciences and Applications 19-24 (2010)
[13] Vaishali V. Somana, V. M. Nanoti, D. K. Kulkarni, Vijay V. Soman, Physics Procedia, 54 , 37,(2014)

